An approximate renormalization-group transformation for Hamiltonian systems with three degrees of freedom

C. Chandre[1], H.R. Jauslin[1], G. Benfatto[2], and A. Celletti[3]

[1] *Laboratoire de Physique-CNRS, Université de Bourgogne, B.P. 47 870, F-21078 Dijon, France*

[2] *Dipartimento di Matematica, Università di Roma "Tor Vergata", Via della Ricerca Scientifica, I-00133 Roma, Italy*

[3] *Dipartimento di Matematica Pura e Applicata, Università di L'Aquila, Via Vetoio, I-67100 L'Aquila, Italy*

We construct an approximate renormalization transformation that combines Kolmogorov-Arnold-Moser (KAM) and renormalization-group techniques, to analyze instabilities in Hamiltonian systems with three degrees of freedom. This scheme is implemented both for isoenergetically nondegenerate and for degenerate Hamiltonians. For the *spiral mean* frequency vector, we find numerically that the iterations of the transformation on nondegenerate Hamiltonians tend to degenerate ones on the critical surface. As a consequence, isoenergetically degenerate and nondegenerate Hamiltonians belong to the same universality class, and thus the corresponding critical invariant tori have the same type of scaling properties. We numerically investigate the structure of the attracting set on the critical surface and find that it is a *strange nonchaotic attractor*. We compute exponents that characterize its universality class.

I. INTRODUCTION

The breakup of invariant tori is one of the key mechanisms of the transition to chaos in Hamiltonian dynamics. For two dimensional systems and for quadratic irrational frequencies, it has been observed that, at the transition, a sequence of periodic orbits approaches geometrically a torus of the given frequency, with a nontrivial scaling behavior [1–3]. This self-similarity has been described in terms of a nontrivial fixed point of a renormalization-group transformation in the case of the golden mean [4–9]. The sequence of periodic orbits responsible for the breakup is generated by the continued fraction expansion of the frequency. For the extension to systems with three degrees of freedom (d.o.f.) involving three incommensurate frequencies, we lack a theory that generalizes the continued fractions. Numerically, three d.o.f. Hamiltonian systems (or equivalently four dimensional volume-preserving maps) have been studied with an extension of Greene's criterion [10–14] and by reconstruction of invariant tori using conjugation theory [15,16]. The conclusion of these analyses was that there is no geometrical accumulation of periodic orbits around the critical torus, and thus absence of universality (at least for the specific frequency vectors they considered).
In Ref. [17], an approximate renormalization-group scheme was described for a reduced family of isoenergetically degenerate Hamiltonians, which is an intermediate case between two and three d.o.f., that in appropriate coordinates can be interpreted as one d.o.f. system driven by two periodic forces with incommensurate frequencies. This was also the class of models considered in Ref. [11,12,14] : They studied an intermediate case between two-dimensional and four-dimensional volume preserving maps. In particular, invariant tori in these intermediate models act as barriers in phase space (limiting the diffusion of trajectories) as for two d.o.f. Hamiltonian systems.

The conclusion of Ref. [17] was that one can still expect *universal* behavior in the breakup of invariant tori: The universality is associated to a hyperbolic nonperiodic attractor of the renormalization flow. The idea is that all Hamiltonians attracted by renormalization to this set will display sequences of scaling factors that appear in a different order but with a universal statistical distribution. The dominant unstable Lyapunov characteristic exponent determines the approach to criticality of the universality class.

By analyzing trajectories on the critical surface, we determine the structure of the critical attractor. Our analysis indicates the existence of a *strange nonchaotic attractor* whose correlation dimension seems to have a value around 1, but it is difficult to analyze it even numerically.

We take the definitions as formulated by Grebogi *et al.* [18]: An attractor of a map is called strange if it is not a finite number of points, nor a piecewise differentiable set. An attractor is chaotic if typical orbits on it have a positive Lyapunov exponent. The strange attractor we obtain is of the same general type as the ones found in Ref. [18,19], for quasiperiodically forced systems (of one and two dimensions). Some of their properties have been rigorously analyzed in Refs. [20–22].

Chaotic attractors for renormalization maps have been conjectured and observed in statistical mechanics [23,24] and dynamical systems [25–28]. In Ref. [29,30], a strange chaotic attractor was found for renormalization of circle maps, and in Ref. [31] similar evidence was found for area-preserving maps, from the scaling analysis of periodic orbits. The origin of randomness in these latter studies is due to the randomness of the sequence of continued fraction approximants for an ensemble of the considered frequencies. In contrast, in the present three d.o.f. case, the rational approximants are a regular sequence, obtained by iteration of a *single* unimodular matrix, which allows us to define a renormalization transformation with a *fixed* frequency vector. We observe that this difference leads to a qualitatively distinct structure of the attractors. Although the geometry of the attractor is singular (i.e., strange), it is not chaotic.

In the present article, we extend the approximate renormalization-group transformation developed in Ref. [17] to a more general family of Hamiltonians with three d.o.f. We find that the renormalization trajectories on the critical surface converge to the reduced family of Hamiltonians considered in Ref. [17].
Similar types of systems were first studied in Ref. [32] with an approximate renormalization scheme that kept less terms than needed to detect an attractor. Instead, their transformation yields a rotation (a center) which is structurally unstable as mentioned in Ref. [32].

We define a renormalization transformation which acts on Hamiltonians with three d.o.f. written in actions $\boldsymbol{A} = (A_1, A_2, A_3) \in \mathbb{R}^3$ and angles $\boldsymbol{\varphi} = (\varphi_1, \varphi_2, \varphi_3) \in \mathbb{T}^3$ (the 3-dimensional torus parametrized, e.g., by $[0, 2\pi]^3$)

$$H(\boldsymbol{A}, \boldsymbol{\varphi}) = H_0(\boldsymbol{A}) + V(\boldsymbol{A}, \boldsymbol{\varphi}), \tag{1.1}$$

where H_0 is the integrable part of the Hamiltonian. We are interested in the stability of the torus with frequency vector $\boldsymbol{\omega}_0$. We suppose that this torus is located at $\boldsymbol{A} = \boldsymbol{0}$ for H_0, i.e., the linear part of H_0 is equal to $\boldsymbol{\omega}_0 \cdot \boldsymbol{A}$. Kolmogorov-Arnold-Moser (KAM) theorems were proven for Hamiltonians (1.1) (with suitable restrictions on the perturbation) provided that H_0 contains a twist in at least one direction in the actions [33], i.e., the Hessian matrix $\partial^2 H_0/\partial \boldsymbol{A}^2$, with elements $\partial^2 H_0/\partial A_i \partial A_j$, is nonzero, and $\boldsymbol{\omega}_0$ satisfies a Diophantine condition. It shows the existence of the torus with frequency vector $\boldsymbol{\omega}_0$ for a sufficiently small and smooth perturbation V. The invariant torus is a small deformation of the unperturbed one. To assume nonzero Hessian matrix, we restrict the family of Hamiltonians (1.1) to the ones with trace one :

$$\operatorname{tr}\left(\frac{\partial^2 H_0}{\partial \boldsymbol{A}^2}\right) = 1. \tag{1.2}$$

The idea is to set up a transformation $\mathcal{R}$ that maps a Hamiltonian H into a rescaled Hamiltonian $\mathcal{R}(H)$, such that irrelevant degrees of freedom are eliminated. The transformation $\mathcal{R}$ should have roughly the following properties: $\mathcal{R}$ has an attractive fixed set (trivial fixed set) of integrable Hamiltonians that have a smooth invariant torus with the frequency $\boldsymbol{\omega}_0$. Every Hamiltonian in its domain of attraction $\mathcal{D}$ has a smooth invariant torus with frequency vector $\boldsymbol{\omega}_0$. The aim is to show that there is another fixed set Λ which lies on the boundary $\partial\mathcal{D}$ (the critical surface) and that is attractive for every Hamiltonian on $\partial\mathcal{D}$.
The transformation $\mathcal{R}$ is defined for a *fixed* frequency vector $\boldsymbol{\omega}_0$ with three incommensurate components. We choose $\boldsymbol{\omega}_0 = (\sigma^2, \sigma, 1)$, where $\sigma \approx 1.3247$ satisfies $\sigma^3 = \sigma + 1$ (named the *spiral mean*). From some of its properties, σ plays a similar role as the golden mean in the two d.o.f. case [34]. The analogy comes from the fact that one can generate rational approximants by iterating a *single* unimodular matrix N. In what follows, we denote *resonance* an element of the sequence $\{\boldsymbol{\nu}_k = N^{k-1}\boldsymbol{\nu}_1, k \geq 1\}$ where $\boldsymbol{\nu}_1 = (1, 0, 0)$ and

$$N = \begin{pmatrix} 0 & 0 & 1 \\ 1 & 0 & 0 \\ 0 & 1 & -1 \end{pmatrix}.$$

The word *resonance* refers to the fact that the small denominators $\boldsymbol{\omega}_0 \cdot \boldsymbol{\nu}_k$ appearing in the perturbation series or in the KAM iteration, tend to zero geometrically as k increases ($\boldsymbol{\omega}_0 \cdot \boldsymbol{\nu}_k = \sigma^{3-k} \to 0$ as $k \to \infty$). We notice that $\boldsymbol{\omega}_0$ is an eigenvector of $\tilde{N}$, where $\tilde{N}$ denotes the transposed matrix of N. The spectrum of $\tilde{N}$ is composed of one real eigenvalue σ^{-1} (with $\boldsymbol{\omega}_0$ as eigenvector), and two complex conjugated eigenvalues $\lambda_1 \pm i\lambda_2 = \sqrt{\sigma}e^{\mp i\alpha}$ (which are of norm larger than one). We denote by $\boldsymbol{\Omega}_\pm = \boldsymbol{\Omega}^{(1)} \pm i\boldsymbol{\Omega}^{(2)}$, the eigenvectors of $\tilde{N}$ associated with these complex eigenvalues.
Our hypothesis (which is also the starting point of a generalization of Greene's criterion in Refs. [11,12]) is that the sequence $\{\boldsymbol{\nu}_k\}$ plays a leading role in the breakup of the invariant torus with frequency vector $\boldsymbol{\omega}_0$.
In this paper, we study the extension of the ideas developed by Escande and Doveil [35–37] to three d.o.f. Hamiltonian systems. We build an approximate scheme by considering the three main resonances $\boldsymbol{\nu}_1$, $\boldsymbol{\nu}_2$, and $\boldsymbol{\nu}_3$. The renormalization focuses on the next smaller scale represented by the resonances $\boldsymbol{\nu}_2$, $\boldsymbol{\nu}_3$, together with $\boldsymbol{\nu}_4 = N\boldsymbol{\nu}_3 = \boldsymbol{\nu}_1 - \boldsymbol{\nu}_3$. It includes a partial elimination of the perturbation (the part which can be considered nonresonant on the smaller scale, namely the mode $\boldsymbol{\nu}_1$), a shift of the resonances, a rescaling of the actions and of the energy, and a translation in the action variables. It is, in spirit, close to the type of transformations considered in Refs. [8,9].
The approximations involved in this scheme are the two main ones used by Escande and Doveil:

a] A quadratic approximation in the actions (as the rescaled Hamiltonian $\mathcal{R}(H)$ is in general higher than quadratic in the actions).

b] A three resonance approximation: we only keep the three main resonances at each iteration of the transformation, i.e., we consider the following family of even Hamiltonians

$$H(\boldsymbol{A}, \boldsymbol{\varphi}) = H_0(\boldsymbol{A}) + \sum_{k=1}^{3} h_k(\boldsymbol{A}) \cos(\boldsymbol{\nu}_k \cdot \boldsymbol{\varphi}), \tag{1.3}$$

where h_k denotes the amplitude of the mode $\boldsymbol{\nu}_k$ of the perturbation.
Hamiltonian (1.1) is isoenergetically nondegenerate if the following determinant of order 4 does not vanish

$$\det \begin{vmatrix} \dfrac{\partial^2 H_0}{\partial \boldsymbol{A}^2} & \dfrac{\partial H_0}{\partial \boldsymbol{A}} \\ \left(\dfrac{\partial H_0}{\partial \boldsymbol{A}}\right)^T & 0 \end{vmatrix} \neq 0. \tag{1.4}$$

On the contrary, if the determinant (1.4) vanishes, H is said to be isoenergetically degenerate. In the following section, we define the renormalization transformation for both cases.

II. RENORMALIZATION TRANSFORMATION

Our transformation is based on the following steps:
1] We apply a canonical transformation that eliminates the first main resonance $\boldsymbol{\nu}_1$. This is performed by a Lie transformation $\mathcal{U}_S : (\boldsymbol{\varphi}, \boldsymbol{A}) \mapsto (\boldsymbol{\varphi}', \boldsymbol{A}')$, generated by a function $S(\boldsymbol{A}, \boldsymbol{\varphi})$. The Hamiltonian expressed in the new coordinates is given by

$$H' = \exp(\hat{S})H \equiv H + \{S, H\} + \frac{1}{2!}\{S, \{S, H\}\} + \cdots,$$

where $\{\, ,\}$ is the Poisson bracket between two scalar functions of the actions and angles:

$$\{f, g\} = \frac{\partial f}{\partial \boldsymbol{\varphi}} \cdot \frac{\partial g}{\partial \boldsymbol{A}} - \frac{\partial f}{\partial \boldsymbol{A}} \cdot \frac{\partial g}{\partial \boldsymbol{\varphi}},$$

and the operator $\hat{S}$ is defined as $\hat{S}H \equiv \{S, H\}$. Denoting by ε the size of h_k, the generating function S is determined by the requirement that the order $O(\varepsilon)$ of the mode $\boldsymbol{\nu}_1$ in H' vanishes:

$$\{S, H_0\} + h_1(\boldsymbol{A}) \cos(\boldsymbol{\nu}_1 \cdot \boldsymbol{\varphi}) = 0.$$

This equation has the solution

$$S(\boldsymbol{A}, \boldsymbol{\varphi}) = S_1(\boldsymbol{A}) \sin(\boldsymbol{\nu}_1 \cdot \boldsymbol{\varphi}),$$

where

$$S_1(\boldsymbol{A}) = -\frac{h_1(\boldsymbol{A})}{\boldsymbol{\omega}(\boldsymbol{A}) \cdot \boldsymbol{\nu}_1}, \quad \boldsymbol{\omega}(\boldsymbol{A}) = \frac{\partial H_0}{\partial \boldsymbol{A}}.$$

This step generates arbitrary orders in the action variables [$\boldsymbol{\omega}(\boldsymbol{A})$ is linear in the actions]. In order to map quadratic Hamiltonians into itself, we expand H' to quadratic order in the actions, and we neglect higher orders. The justification for this approximation is that, as the torus is located at $\boldsymbol{A} = \boldsymbol{0}$ for H_0, one can expect that for small ε, it is close to $\boldsymbol{A} = \boldsymbol{0}$. We notice that $h_2(\boldsymbol{A})$ and $h_3(\boldsymbol{A})$ are not changed up to order $O(\varepsilon^3)$. Furthermore, we neglect all the Fourier modes except $\boldsymbol{0}$, $\boldsymbol{\nu}_2$, $\boldsymbol{\nu}_3$, and $\boldsymbol{\nu}_4$, and all terms of order greater than 3 in ε. This leads to the expression of H':

$$\begin{aligned} H' = \; & H_0 + h_2 \cos(\boldsymbol{\nu}_2 \cdot \boldsymbol{\varphi}) + h_3 \cos(\boldsymbol{\nu}_3 \cdot \boldsymbol{\varphi}) \\ & + \frac{1}{2}\langle \{S, h_1 \cos(\boldsymbol{\nu}_1 \cdot \boldsymbol{\varphi})\}\rangle + \{S, h_3 \cos(\boldsymbol{\nu}_3 \cdot \boldsymbol{\varphi})\}, \end{aligned} \tag{2.1}$$

where $\langle\,\rangle$ denotes the mean value defined as

$$\langle h \rangle(\boldsymbol{A}) = \int_{\mathbb{T}^3} h(\boldsymbol{A}, \boldsymbol{\varphi}) \frac{d^3\boldsymbol{\varphi}}{(2\pi)^3}.$$

The last term of Eq. (2.1) contains the Fourier mode $\boldsymbol{\nu}_4 = \boldsymbol{\nu}_1 - \boldsymbol{\nu}_3$ of amplitude

$$h_4(\boldsymbol{A}) = \frac{1}{2}\left(S_1 \boldsymbol{\nu}_1 \cdot \frac{\partial h_3}{\partial \boldsymbol{A}} + h_3 \boldsymbol{\nu}_3 \cdot \frac{\partial S_1}{\partial \boldsymbol{A}}\right). \tag{2.2}$$

We expand h_4 to quadratic order in the actions.
2] From Eq. (2.1), the mean value term $\langle \{S, h_1 \cos(\boldsymbol{\nu}_1 \cdot \boldsymbol{\varphi})\}\rangle$ produces a linear term in the actions. In order that the mean value of the linear term in H' becomes $\boldsymbol{\omega}_0 \cdot \boldsymbol{A}$, we eliminate this term by a translation in the actions $\boldsymbol{A} \mapsto \boldsymbol{A} + \boldsymbol{a}$, where $\boldsymbol{a}$ is of order $O(\varepsilon^2)$ (so it does not produce any other effect up to the second order in ε).
3] We shift the resonances $\boldsymbol{\nu}_k \mapsto \boldsymbol{\nu}_{k-1}$: We require that the new angles satisfy $\cos(\boldsymbol{\nu}_{k+1} \cdot \boldsymbol{\varphi}) = \cos(\boldsymbol{\nu}_k \cdot \boldsymbol{\varphi}')$, for $k = 1, 2, 3$. This is performed by the linear canonical transformation

$$(\boldsymbol{A}, \boldsymbol{\varphi}) \mapsto (N^{-1}\boldsymbol{A}, \tilde{N}\boldsymbol{\varphi}).$$

We notice that N is an integer matrix with determinant one. Therefore, this transformation preserves the $\mathbb{T}^3$-structure of the angles. This step changes the frequency $\boldsymbol{\omega}_0$ into $\tilde{N}\boldsymbol{\omega}_0 = \sigma^{-1}\boldsymbol{\omega}_0$ (since $\boldsymbol{\omega}_0$ is an eigenvector of $\tilde{N}$ by construction).
4] We rescale the energy (or equivalently the time) by a factor σ, in order to keep the frequency fixed at $\boldsymbol{\omega}_0$.
5] We rescale the actions:

$$H''(\boldsymbol{A}, \boldsymbol{\varphi}) = \lambda H'\left(\frac{\boldsymbol{A}}{\lambda}, \boldsymbol{\varphi}\right),$$

such that Condition (1.2) is satisfied for H''. This normalization condition is essential to the convergence of the transformation.
Similar type of approximate renormalization transformations has been defined in Ref. [32]. The main difference is that they used a normalization condition such that the Hessian matrix $\partial^2 H_0/\partial \boldsymbol{A}^2$ is of rank 2, instead of Condition (1.2). Below, we make the distinction between degenerate and nondegenerate Hamiltonians: we explicit the renormalization transformation in both cases.

A. Isoenergetically degenerate Hamiltonians

The renormalization transformation described in this section was derived in Ref. [17]. The integrable part H_0 is given by

$$H_0(\boldsymbol{A}) = \boldsymbol{\omega}_0 \cdot \boldsymbol{A} + \frac{1}{2}(\boldsymbol{\Omega}\cdot\boldsymbol{A})^2, \tag{2.3}$$

where $\boldsymbol{\Omega}$ is a free vector of norm one: $\|\boldsymbol{\Omega}\| = \left(|\Omega_1|^2+|\Omega_2|^2+|\Omega_3|^2\right)^{1/2} = 1$. In that case, the Hessian matrix $\partial^2 H_0/\partial \boldsymbol{A}^2$ is of rank one (proportional to the projection operator on the $\boldsymbol{\Omega}$-direction); thus the isoenergetic determinant (1.4) is zero. The relevant direction (where there is a twist) in the actions is $\boldsymbol{\Omega}$. We expand $h_k(\boldsymbol{A})$ in the $(\boldsymbol{\Omega}\cdot\boldsymbol{A})$-variable:

$$h_k(\boldsymbol{A}) = f_k + g_k\boldsymbol{\Omega}\cdot\boldsymbol{A} + \frac{1}{2}m_k(\boldsymbol{\Omega}\cdot\boldsymbol{A})^2. \tag{2.4}$$

We rewrite the meanvalue terms in H' of Eq. (2.1) as

$$\begin{aligned} H_0(\boldsymbol{A}) &+ \frac{1}{2}\langle\{S, h_1\cos(\boldsymbol{\nu}_1\cdot\boldsymbol{\varphi})\}\rangle \\ &= H_0(\boldsymbol{A}) + \frac{1}{4}\boldsymbol{\nu}_1\cdot\frac{\partial}{\partial\boldsymbol{A}}(S_1 h_1) \\ &= \boldsymbol{\omega}_0\cdot\boldsymbol{A} + a\boldsymbol{\Omega}\cdot\boldsymbol{A} + \frac{1}{2}(1+\mu)(\boldsymbol{\Omega}\cdot\boldsymbol{A})^2 + \text{const.} \end{aligned}$$

The linear term $a\boldsymbol{\Omega}\cdot\boldsymbol{A}$ is eliminated by a translation in the actions $\boldsymbol{A}' = \boldsymbol{A} + \boldsymbol{\Omega}a/(1+\mu)$.
The shift of the resonances (Step 3) changes the vector $\boldsymbol{\Omega}$ into $\tilde{N}\boldsymbol{\Omega}$. In order to keep a unit norm, we define the image of $\boldsymbol{\Omega}$ by

$$\boldsymbol{\Omega}' = \frac{\tilde{N}\boldsymbol{\Omega}}{\|\tilde{N}\boldsymbol{\Omega}\|}. \tag{2.5}$$

The quadratic term of the integrable part of H' becomes $\sigma\|\tilde{N}\boldsymbol{\Omega}\|^2(1+\mu)(\boldsymbol{\Omega}'\cdot\boldsymbol{A})^2/2$. We rescale the actions (Step 5) by a factor

$$\lambda = \sigma\|\tilde{N}\boldsymbol{\Omega}\|^2(1+\mu), \tag{2.6}$$

such that H_0 is mapped into

$$H_0'(\boldsymbol{A}) = \boldsymbol{\omega}_0\cdot\boldsymbol{A} + \frac{1}{2}(\boldsymbol{\Omega}'\cdot\boldsymbol{A})^2,$$

with $\boldsymbol{\Omega}'$ given by Eq. (2.5). The transformation is thus equivalent to a mapping acting on an 11-dimensional space (recall that $\boldsymbol{\Omega}$ and $\boldsymbol{\Omega}'$ have unit norm)

$$(\{f_k, g_k, m_k\}_{k=1,2,3};\boldsymbol{\Omega}) \mapsto (\{f_k', g_k', m_k'\}_{k=1,2,3};\boldsymbol{\Omega}'),$$

defined by the following relations

$$f_k' = \sigma^2\|\tilde{N}\boldsymbol{\Omega}\|^2(1+\mu)f_{k+1}, \tag{2.7}$$
$$g_k' = \sigma\|\tilde{N}\boldsymbol{\Omega}\|g_{k+1}, \tag{2.8}$$
$$m_k' = \frac{1}{1+\mu}m_{k+1} \qquad \text{for } k=1,2 \tag{2.9}$$
$$f_3' = \sigma^2\|\tilde{N}\boldsymbol{\Omega}\|^2(1+\mu)h_4^{(0)}, \tag{2.10}$$
$$g_3' = \sigma\|\tilde{N}\boldsymbol{\Omega}\|h_4^{(1)}, \tag{2.11}$$
$$m_3' = \frac{2}{1+\mu}h_4^{(2)}, \tag{2.12}$$

where $h_4^{(i)}$ is the coefficient in $(\boldsymbol{\Omega}\cdot\boldsymbol{A})^i$ of h_4 given by Eq. (2.2). Denoting by

$$\beta_1 = \frac{\boldsymbol{\Omega}\cdot\boldsymbol{\nu}_1}{\boldsymbol{\omega}_0\cdot\boldsymbol{\nu}_1} = \frac{\Omega_1}{\sigma^2},$$

and

$$\beta_3 = \frac{\boldsymbol{\Omega}\cdot\boldsymbol{\nu}_3}{\boldsymbol{\omega}_0\cdot\boldsymbol{\nu}_1} = \frac{\Omega_3}{\sigma^2},$$

we obtain explicit expressions for μ and $h_4^{(i)}$ of the renormalization map:

$$\begin{aligned} \mu &= \frac{3}{2}\beta_1(g_1-\beta_1 f_1)(\beta_1 g_1 - \beta_1^2 f_1 - m_1), \\ h_4^{(0)} &= -\frac{1}{2}\left[\beta_3 f_3(g_1-\beta_1 f_1) + \beta_1 f_1 g_3\right], \\ h_4^{(1)} &= -\frac{1}{2}\left[((\beta_1+\beta_3)g_3 - 2\beta_1\beta_3 f_3)(g_1-\beta_1 f_1)\right. \\ &\qquad \left. +\beta_1 f_1 m_3 + \beta_3 f_3 m_1\right], \\ h_4^{(2)} &= -\frac{1}{2}\left[((\beta_1+\beta_3/2)m_3 - \beta_1(\beta_1+2\beta_3)g_3 + 3\beta_1^2\beta_3 f_3)\right. \\ &\qquad \times(g_1-\beta_1 f_1) \\ &\qquad \left. +(\beta_1/2+\beta_3)m_1 g_3 - 3\beta_1\beta_3 m_1 f_3/2\right]. \end{aligned}$$

Iterating the renormalization map, Eq. (2.5) reduces to a rotation; in fact, as $\boldsymbol{\omega}_0$ is an eigenvector of $\tilde{N}$ with an eigenvalue of norm smaller than one, the $\boldsymbol{\omega}_0$-direction of the vector $\boldsymbol{\Omega}$ is contracted. The renormalization transformation reduces to a 10-dimensional map, where the vector $\boldsymbol{\Omega}$ rotates in the plane $(\boldsymbol{\Omega}^{(1)}, \boldsymbol{\Omega}^{(2)})$. It is thus parametrized by an angle θ defined by

$$\boldsymbol{\Omega} = \rho(\boldsymbol{\Omega}^{(1)}\cos\theta + \boldsymbol{\Omega}^{(2)}\sin\theta).$$

If we choose $\boldsymbol{\Omega}^{(i)}$ such that

$$\begin{aligned} \boldsymbol{\Omega}^{(1)} &= (\sigma^{-1/2}\cos\alpha, 1, \sigma^{1/2}\cos\alpha), \\ \boldsymbol{\Omega}^{(2)} &= (\sigma^{-1/2}\sin\alpha, 0, -\sigma^{1/2}\sin\alpha), \end{aligned}$$

where $\lambda_1 \pm i\lambda_2 = \sigma^{1/2}e^{\mp i\alpha}$ are the two complex conjugated eigenvalues of N, the expression of $\boldsymbol{\Omega}$ becomes

$$\boldsymbol{\Omega} = \rho(\sigma^{-1/2}\cos(\alpha-\theta), \cos\theta, \sigma^{1/2}\cos(\alpha+\theta)),$$

where, since $\|\boldsymbol{\Omega}\| = 1$, $\rho = [F(\theta)]^{-1/2}$, and

$$F(\theta) = \sigma^{-1}\cos^2(\alpha-\theta) + \cos^2\theta + \sigma\cos^2(\alpha+\theta). \tag{2.13}$$

The parameters β_1 and β_3 are expressed as functions of θ:

$$\begin{aligned} \beta_1 &= \sigma^{-5/2}\frac{\cos(\alpha-\theta)}{[F(\theta)]^{1/2}}, \\ \beta_3 &= \sigma^{-3/2}\frac{\cos(\alpha+\theta)}{[F(\theta)]^{1/2}}. \end{aligned}$$

The expression of the norm $\|\tilde{N}\boldsymbol{\Omega}\|$ is given by

$$\|\tilde{N}\boldsymbol{\Omega}\| = \left(\sigma\frac{F(\alpha+\theta)}{F(\theta)}\right)^{1/2}.$$

B. General quadratic Hamiltonians

For the most general quadratic Hamiltonians, we consider the family

$$H(\boldsymbol{A},\boldsymbol{\varphi}) = f(\boldsymbol{\varphi}) + [\boldsymbol{\omega}_0 + \boldsymbol{g}(\boldsymbol{\varphi})]\cdot\boldsymbol{A} + \frac{1}{2}\boldsymbol{A}\cdot[M + m(\boldsymbol{\varphi})]\boldsymbol{A}, \tag{2.14}$$

where M and m are 3×3 symmetric matrices, and $\boldsymbol{g}$ is a vector. The matrix M is assumed to be nonzero (its trace is equal to one) and $\boldsymbol{g}$ is not parallel to $\boldsymbol{\omega}_0$. In Step 3, the vector $\boldsymbol{g}$ is renormalized into $\tilde{N}\boldsymbol{g}$. Thus the iterations of $\tilde{N}$ converge to the plane defined by $\boldsymbol{\Omega}^{(1)}$ and $\boldsymbol{\Omega}^{(2)}$, i.e., the $\boldsymbol{\omega}_0$-direction of the perturbation is contracted (as the modulus of the eigenvalue associated with $\boldsymbol{\omega}_0$ is lower than one). In H_0, except the term $\boldsymbol{\omega}_0\cdot\boldsymbol{A}$ which is kept fixed by renormalization, in all the other terms of higher order in $\boldsymbol{A}$, the $\boldsymbol{\omega}_0$-direction is also contracted. Notice that the quadratic term can be written as

$$\frac{1}{2}\boldsymbol{A}\cdot M\boldsymbol{A} = \frac{1}{2}\sum_{i,j=1,2,3} m_0^{(i,j)}(\boldsymbol{\Omega}^{(i)}\cdot\boldsymbol{A})(\boldsymbol{\Omega}^{(j)}\cdot\boldsymbol{A}),$$

where $\boldsymbol{\Omega}^{(3)} = \boldsymbol{\omega}_0$, and $\boldsymbol{\Omega}^{(1)}$ and $\boldsymbol{\Omega}^{(2)}$ are the real and imaginary part of the eigenvectors $\boldsymbol{\Omega}_\pm$ of $\tilde{N}$. Then it is sufficient to consider perturbations which only depend on the variables $(\boldsymbol{\Omega}^{(1)}\cdot\boldsymbol{A})$ and $(\boldsymbol{\Omega}^{(2)}\cdot\boldsymbol{A})$, and an integrable part H_0 of the form

$$H_0(\boldsymbol{A}) = \boldsymbol{\omega}_0\cdot\boldsymbol{A} + \frac{1}{2}\sum_{i,j=1,2} m_0^{(i,j)}(\boldsymbol{\Omega}^{(i)}\cdot\boldsymbol{A})(\boldsymbol{\Omega}^{(j)}\cdot\boldsymbol{A}), \tag{2.15}$$

where $\boldsymbol{\Omega}^{(i)}$ is a fixed vector (real or imaginary part of the complex eigenvectors of $\tilde{N}$), and the matrix m_0, with elements $m_0^{(i,j)}$, is symmetric and will be a variable of the renormalization map with the restriction that the trace of the Hessian matrix is equal to one. There are two directions $\boldsymbol{\Omega}^{(1)}$ and $\boldsymbol{\Omega}^{(2)}$ of twist in the actions. The Hessian matrix is noninvertible, but, in general, the isoenergetic determinant (1.4) is nonzero. We write h_k, for $k=1,2,3$, in the $(\boldsymbol{\Omega}^{(i)}\cdot\boldsymbol{A})$-variables:

$$h_k(\boldsymbol{A}) = f_k + \sum_{i=1,2} g_k^{(i)}(\boldsymbol{\Omega}^{(i)}\cdot\boldsymbol{A}) + \frac{1}{2}\sum_{i,j=1,2} m_k^{(i,j)}(\boldsymbol{\Omega}^{(i)}\cdot\boldsymbol{A})(\boldsymbol{\Omega}^{(j)}\cdot\boldsymbol{A}), \tag{2.16}$$

where the matrices m_k, whose elements are $m_k^{(i,j)}$, are symmetric. We expand h_4 given by Eq. (2.2) such that Eq. (2.16) defines also the coefficients of the Taylor expansion of h_4. The shift of the resonances (Step 3) changes $\boldsymbol{\Omega}^{(1)}$ and $\boldsymbol{\Omega}^{(2)}$ into

$$\tilde{N}\boldsymbol{\Omega}^{(1)} = \lambda_1\boldsymbol{\Omega}^{(1)} - \lambda_2\boldsymbol{\Omega}^{(2)},$$
$$\tilde{N}\boldsymbol{\Omega}^{(2)} = \lambda_2\boldsymbol{\Omega}^{(1)} + \lambda_1\boldsymbol{\Omega}^{(2)}.$$

This is equivalent to a rotation in the plane $(\boldsymbol{\Omega}^{(1)},\boldsymbol{\Omega}^{(2)})$ combined with an amplification by a factor $(\lambda_1^2+\lambda_2^2)^{1/2} = \sqrt{\sigma}$. This step changes the matrix m_k into m_k' whose elements are

$$\begin{aligned}
m_k'^{(1,1)} &= \lambda_1^2 m_k^{(1,1)} + 2\lambda_1\lambda_2 m_k^{(1,2)} + \lambda_2^2 m_k^{(2,2)},\\
m_k'^{(1,2)} &= m_k'^{(2,1)}\\
&= -\lambda_1\lambda_2 m_k^{(1,1)} + (\lambda_1^2-\lambda_2^2)m_k^{(1,2)} + \lambda_1\lambda_2 m_k^{(2,2)},\\
m_k'^{(2,2)} &= \lambda_2^2 m_k^{(1,1)} - 2\lambda_1\lambda_2 m_k^{(1,2)} + \lambda_1^2 m_k^{(2,2)}.
\end{aligned}$$

The matrix m_0 is changed into m_0' according to the same formulae. The vector $\boldsymbol{g}_k = (g_k^{(1)}, g_k^{(2)})$ is mapped into $\boldsymbol{g}_k' = (g_k'^{(1)}, g_k'^{(2)})$ whose elements are

$$\begin{aligned}
g_k'^{(1)} &= \lambda_1 g_k^{(1)} + \lambda_2 g_k^{(2)},\\
g_k'^{(2)} &= -\lambda_2 g_k^{(1)} + \lambda_1 g_k^{(2)}.
\end{aligned}$$

The rotation (under the action of $\tilde{N}$) of $\boldsymbol{g}_k$ and m_k is analogous to the rotation of $\boldsymbol{\Omega}$ [see Eq. (2.5)]; the amplification is compensated by the rescaling of the actions to avoid divergences of the transformation. We rewrite the mean-value term in H' as

$$\langle\{S, h_1\cos(\boldsymbol{\nu}_1\cdot\boldsymbol{\varphi})\}\rangle = \text{const} + \sum_{i=1,2} a^{(i)}\boldsymbol{\Omega}^{(i)}\cdot\boldsymbol{A} + \sum_{i,j=1,2}\mu^{(i,j)}(\boldsymbol{\Omega}^{(i)}\cdot\boldsymbol{A})(\boldsymbol{\Omega}^{(j)}\cdot\boldsymbol{A}).$$

The linear terms $a^{(i)}\boldsymbol{\Omega}^{(i)}\cdot\boldsymbol{A}$ are eliminated by a translation in the actions. The mean-value of the quadratic part of H' is $\sum_{i,j=1,2}\sigma(m_0'^{(i,j)}+\mu^{(i,j)})(\boldsymbol{\Omega}^{(i)}\cdot\boldsymbol{A})(\boldsymbol{\Omega}^{(j)}\cdot\boldsymbol{A})/2$, and thus the new Hessian matrix is given by $\sum_{i,j=1,2}\sigma(m_0'^{(i,j)}+\mu^{(i,j)})\boldsymbol{\Omega}^{(i)}\otimes\boldsymbol{\Omega}^{(j)}$, where the elements of the matrix $\boldsymbol{\Omega}^{(i)}\otimes\boldsymbol{\Omega}^{(j)}$ are $(\boldsymbol{\Omega}^{(i)}\otimes\boldsymbol{\Omega}^{(j)})_{kl} = \Omega_k^{(i)}\Omega_l^{(j)}$. In order to have the trace of the Hessian matrix of the rescaled Hamiltonian equal to one, we rescale the actions (Step 5) by a factor

$$\lambda = \sigma\sum_{i,j=1,2}(m_0'^{(i,j)}+\mu^{(i,j)})\mathrm{tr}(\boldsymbol{\Omega}^{(i)}\otimes\boldsymbol{\Omega}^{(j)}).$$

The approximate transformation is equivalent to a mapping acting on a 20-dimensional space (since the matrices m are symmetric and m_0 has a constant trace):

$$(\{f_k, g_k^{(i)}, m_k^{(i,j)}, m_0^{(i,j)}\}_{k=1,2,3;i,j=1,2}) \mapsto (\{f_k'', g_k''^{(i)}, m_k''^{(i,j)}, m_0''^{(i,j)}\}_{k=1,2,3;i,j=1,2}),$$

defined by the following relations

$$\begin{aligned}
f_k'' &= \lambda\sigma f_{k+1},\\
g_k''^{(i)} &= \sigma g_{k+1}'^{(i)},\\
m_k''^{(i,j)} &= \frac{\sigma}{\lambda} m_{k+1}'^{(i,j)},\\
m_0''^{(i,j)} &= \frac{\sigma}{\lambda} m_0'^{(i,j)},
\end{aligned}$$

for $k=1,2,3$ and $i,j=1,2$.

III. RENORMALIZATION FLOW

For each scheme (Secs. II A and II B), the numerical implementation shows that there are two main domains separated by a *critical surface*: one where the iteration converges towards a family of integrable Hamiltonians (trivial fixed set), and the other where it diverges to infinity.

A. Reduction to degenerate Hamiltonians

As a first result, we numerically observe that the transformation acting on nondegenerate Hamiltonians considered in Sec. II B tends to the degenerate ones of Sec. II A, *on the critical surface*. More precisely, if we consider Hamiltonians (2.14) with M of rank 3, the contraction in the $\boldsymbol{\omega}_0$-direction, as explained in Sec. II B, reduces the rank of M by one; the 3×3 matrix M is thus reduced to a 2×2 matrix m_0. Furthermore the numerical results show that the renormalization reduces this rank to one when we iterate on the critical surface. Figure 1 shows the evolution, under the renormalization map, of the determinant of m_0. The upper curve corresponds to a starting Hamiltonian in the domain of attraction of the trivial fixed set, and the lower one corresponds to iterations on the critical surface (both evolutions start with the same quadratic part). We also check that the determinant of the matrices m_k tends to zero. Furthermore, the directions of the vectorial parameters ($\boldsymbol{g}$ and m) tend to be aligned by the iteration : Hamiltonians (2.16) tend to Hamiltonians (2.4), and Hamiltonian (2.15) tends to Hamiltonian (2.3), all with a same direction $\boldsymbol{\Omega}$. In order to characterize this, we define $\boldsymbol{\Omega}$ as the unit vector with the same direction as $\boldsymbol{g}_1$. We compute the norm of $\boldsymbol{\Omega}_2-\boldsymbol{\Omega}$ and $\boldsymbol{\Omega}_3-\boldsymbol{\Omega}$, where $\boldsymbol{\Omega}_2$ (resp. $\boldsymbol{\Omega}_3$) is a unit vector with direction $\boldsymbol{g}_2$ (resp. $\boldsymbol{g}_3$). Moreover, in order to see that the quadratic terms are proportional to $\boldsymbol{\Omega}\otimes\boldsymbol{\Omega}$, we compute the norm of $m_0-c\boldsymbol{\Omega}\otimes\boldsymbol{\Omega}$ where c is defined by the constant trace of m_0 (similar calculations have been done for the other matrices m_k). These differences tend to zero as we iterate a Hamiltonian on the critical surface (they are of order 10^{-5} after 20 iterations on the critical surface).
From these observations, we conclude that isoenergetically degenerate and nondegenerate Hamiltonians belong to the same universality class. According to the general renormalization-group picture, the corresponding critical invariant tori are predicted to have the same type of scaling properties.
We lack an explanation of the mechanism of this second reduction of the rank. We remark that this second reduction is not just an effect of the rescaling (steps 3 to 5) as it is the case for the $\boldsymbol{\omega}_0$-contraction : the second reduction does not happen outside the critical surface. We conjecture that this reduction will also occur in an exact renormalization scheme, but this point has not yet been explored.
We remark that the choice of the normalization condition (1.2) seems essential to obtain a nontrivial attractor. Other choices [32], like $\det m_0 = 1$, do not lead to a critical attractor and the iterations appear to diverge on the critical surface (one eigenvalue of m_0 tends to zero and the other one to infinity).
The reduction to rank one allows us to work, for the precise analysis of the attractor, with the data obtained for the degenerate case (Sec. II A).

B. Trivial attractor

The domain of attraction of the trivial fixed set is the domain where the perturbation of the iterated Hamiltonians tends to zero. However, the renormalization trajectories in this domain do not converge to a fixed Hamiltonian but converge to a *smooth quasiperiodic* set of integrable Hamiltonians. This can be explained by looking at the map (2.5). The eigenvalues of $\tilde{N}$ are σ^{-1} and $\sqrt{\sigma}e^{\pm i\alpha}$ where $\alpha \approx 2\pi\times 0.3880$ ($\alpha = \arccos(-\sigma^{3/2}/2)$). The map (2.5) leads asymptotically to a rotation of angle α in the plane $(\boldsymbol{\Omega}^{(1)},\boldsymbol{\Omega}^{(2)})$, after a contraction in the $\boldsymbol{\omega}_0$-direction, as explained in Sec. II A. The values of the rescalings (2.6) at the trivial fixed set are given by a smooth function of θ. It is given explicitely by

$$\lambda(\theta)=\sigma^2\frac{F(\alpha+\theta)}{F(\theta)},$$

where F is given by Eq. (2.13). This trivial rescaling curve is depicted in Fig. 2. Since $\alpha/2\pi$ is close to 7/18, the evolution of λ oscillates approximately with period 18.

C. Critical attractor

On the critical surface, the renormalization flow converges to an attracting set. This set has a codimension 1 stable manifold, i.e., one expansive direction transverse to the critical surface. This set plays, for the system we consider, the same role as the nontrivial fixed point of the renormalization-group transformation for quadratic irrational frequencies in two d.o.f. Hamiltonian systems. In particular, its existence implies *universality* for one-parameter families crossing the critical surface. Different trajectories of the transformation display the same values of the rescalings with a different order but with a *universal* statistical distribution. We define exponents that characterize the universality class associated with the spiral mean. The mean-rescaling is defined by $\lambda=\lim_{n\to\infty}\left(\prod_{j=1}^{n}\lambda_j\right)^{1/n}$, where λ_j is the value of the rescaling after j iterations on the critical surface. We also calculate the largest Lyapunov exponent κ which measures the approach to criticality as a function of the coupling constant, of the universality class. The result we found is that these limits do not depend on the Hamiltonian on the critical surface where we start the iteration nor on the initial choice of $\boldsymbol{\Omega}$. The coefficients κ and λ depend only on $\boldsymbol{\omega}_0$. Numerically, we find $\kappa \approx 0.6427$ and $\lambda \approx 3.1479$.

We provide numerical evidence that this attractor is strange and nonchaotic. We remark that Eqs. (2.7)-(2.12) of the renormalization map have the form of a nonlinear system $\{f_k, g_k, m_k\}$ (for $k = 1, 2, 3$) driven by a quasiperiodic variable $\theta \mapsto \theta + \alpha$, given by the evolution of the vector $\boldsymbol{\Omega}$ represented by Eq. (2.5). This type of systems has been analyzed in Refs. [18–22], where one of the main conclusion is the existence of strange nonchaotic attractors. In order to analyze the nontrivial attractor from this perspective, we show in Fig. 2 a two-dimensional plot of the time series (θ_j, λ_j) of the scaling factor λ_j, and the angle θ_j, where j is the index of the iteration on the attractor. This figure shows that λ appears to be a continuous (one to one) function of θ. The evolution of the rescaling λ_j displays an approximate period 18 behavior, similar to the one observed on the trivial attractor. We remark that for the trivial attractor $\lambda(\theta)$ is smooth, while for the critical attractor $\lambda(\theta)$ has a set of cusps (nondifferentiable points). Since the driving map $\theta_{j+1} = \theta_j + \alpha$ fills the circle densely, and the renormalization map is smooth, the function $\lambda(\theta)$ must have a dense set of cusps. In Fig. 3, we show the corresponding plot for the parameter g_1. This picture is the renormalization trajectory of a single initial Hamiltonian on the attractor. It shows that $g_1(\theta)$ is not a single valued function of θ. Similar pictures are obtained for the other coordinates of the map.

In order to analyze the structure of the attractor in more detail, we consider it from a different point of view: We take a set of initial conditions on the critical surface (not on the attractor) parametrized by an angle θ varying over a small interval $[\theta_1, \theta_2]$. Figure 4a shows the projection of this segment on the plane (θ, g_1). Figure 4b shows the image of the projection after 100 iterations, and Fig. 4c after 350 iterations. This shows that as the segment comes closer to the attractor the number of steep oscillations becomes larger, suggesting that in the limit they correspond to discontinuities of the attractor. This behavior is similar to the observations of Ref. [18] and is compatible with the results of Ref. [22]. These oscillations are associated to abrupt changes of the signs of the coordinates. One can conjecture that on the attractor, there is an infinite number of such changes of sign. The same kind of phenomena is observed for the other coordinates. In order to see the effect of these changes of sign in the renormalization dynamics on the attractor, we compare in Fig. 5 the power spectrum of the time series of g_1, with the one of $|g_1|$. The second one indicates that the behavior of $|g_1|$ is very close to quasiperiodic (with frequencies 1 and $\alpha/2\pi$), while g_1 shows a broad spectrum.

A further insight into the structure of the attractor can be obtained by following the trajectories for a single initial θ and a set of different choices of the other coordinates at a given "time" (i.e., after a fixed number of iterations of the map). After the relaxation transient, one observes that all initial points fall into one of eight points of the attractor (in the example of Ref. [18], there are two such limiting points). The iteration of these eight points generates eight branches of the attractor that are not completely disjoint. In order to visualize these eight branches, we display in Fig. 6 the values of an observable $\mathcal{B}$ that allows to distinguish them. A suitable choice is the weighted sum of the coordinates of $\boldsymbol{x} = (x_1, \ldots, x_9)$

$$\mathcal{B}(\boldsymbol{x}) = \sum_{i=1}^{9} \frac{x_i}{\eta_i},$$

with

$$\eta_i = \lim_{N\to\infty} \frac{1}{N} \sum_{j=1}^{N} |x_i(j)|,$$

where $x_i(j)$ is the j-th iterate of an initial condition of the coordinate x_i. These branches are related by symmetry, as described in Sec. III D.

In summary, the numerical results suggest the following characterization of the attractor: It is a set composed of eight branches that differ only in the signs of one or more h_k (the amplitude of the Fourier mode $\boldsymbol{\nu}_k$). Each of the branches has a dense set of discontinuities. It seems to be an example in 9 dimensions of the type of attractors described in Ref. [18].

In order to characterize the singularities, we compute the correlation dimension of the attractor according to the method developed by Grassberger and Procaccia [38,39]. We did not find a clear result, but there is some evidence that the dimension has a value around 1, in agreement with Figs. 3 and 6, and with the projection of the attractor on the plane (g_1, m_1) depicted in Fig. 7.

D. Symmetries of the transformation

In this paper, we have considered only even perturbations, i.e., such that the Fourier modes are only cosine terms. The results can be extended to the more general case, including non-even modes $\boldsymbol{\nu}_k$ $(k = 1, 2, 3)$, by the following symmetry arguments [40,7]. These arguments allow also to understand the relation between the eight branches of the attractor.

We analyze the effect of a shift of the origin of the angles on the renormalization transformation. We denote this shift as

$$\mathcal{T}_{\boldsymbol{\theta}} : \boldsymbol{\varphi} \mapsto \boldsymbol{\varphi} + \boldsymbol{\theta}.$$

The KAM transformation (Step 1) commutes with $\mathcal{T}_{\boldsymbol{\theta}}$. The action of $\mathcal{T}_{\boldsymbol{\theta}}$ on the shift of the resonances (Step 3) is characterized by the following intertwinning relation [41]:

$$\mathcal{R} \circ \mathcal{T}_{\boldsymbol{\theta}} = \mathcal{T}_{\tilde{N}\boldsymbol{\theta}} \circ \mathcal{R}, \tag{3.1}$$

where $\mathcal{R}$ denotes the renormalization transformation. Applying this relation to the critical attractor gives the relation between the renormalization trajectories for Hamiltonians $H(\boldsymbol{A}, \boldsymbol{\varphi})$ and the ones for Hamiltonians $H(\boldsymbol{A}, \boldsymbol{\varphi} + \boldsymbol{\theta})$. With this type of shift, any Hamiltonian containing only the three modes $\boldsymbol{\nu}_k$, $k = 1, 2, 3$ (with sine and cosine terms), can be put into a cosine representation. Thus the attractors for these models are directly linked by symmetries to the attractor found in the even case.

The eight branches of the critical attractor are mapped into each other by symmetries of this type, realized by shifts in the origin of the angles by $\boldsymbol{\theta}_k = \pi \boldsymbol{\nu}_k$. This corresponds to the eight possible choices of the signs of the three modes.

IV. CONCLUSION

This paper provides numerical results indicating that for the spiral mean frequency vector, the critical surface of the approximate renormalization transformation is the codimension 1 stable manifold of a *strange nonchaotic attractor*. This feature depends strongly on the characteristics of the eigenvalues of N. Moreover, the numerical results suggest that the renormalization transformation can be reduced to an isoenergetically degenerate family of Hamiltonians at criticality. These remarks give new insights for the setup of a systematic renormalization transformation, in the spirit of Refs. [41,8,9].

ACKNOWLEDGMENTS

We acknowledge useful discussions with J.P. Eckmann, G. Gallavotti, H. Koch, J. Laskar, and R.S. MacKay. Support from EC Contract No. ERBCHRXCT94-0460 for the project "Stability and Universality in Classical Mechanics" is acknowledged.

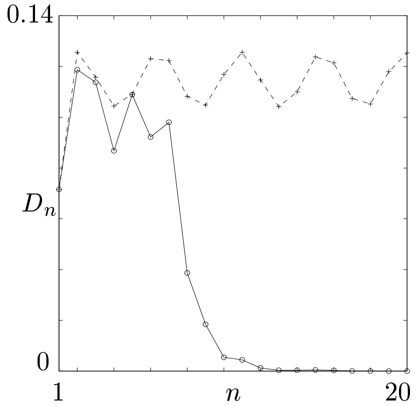

FIG. 1. Evolution of the determinant D_n of the matrix m_0 (as a function of the number of iterations n) : the continuous line is for a trajectory of the renormalization transformation on the critical surface, and the dashed line is for a trajectory inside the domain of attraction of the trivial fixed set.

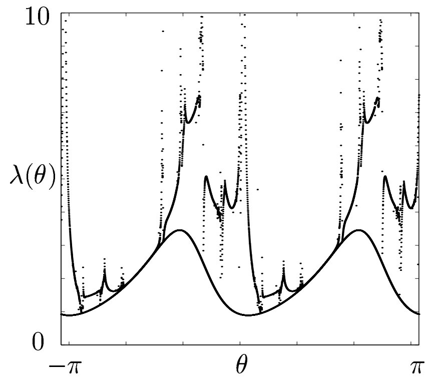

FIG. 2. Values of the rescalings λ as a function of the angle θ between $\boldsymbol{\Omega}$ and $\boldsymbol{\Omega}^{(1)}$ in the $(\boldsymbol{\Omega}^{(1)}, \boldsymbol{\Omega}^{(2)})$-plane. The regular curve is for the trivial fixed set, and the singular curve is for the nontrivial fixed set.

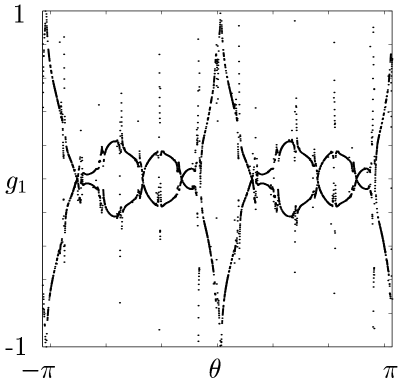

FIG. 3. Values of g_1 as a function of the angle θ, on the critical attractor of the renormalization map.

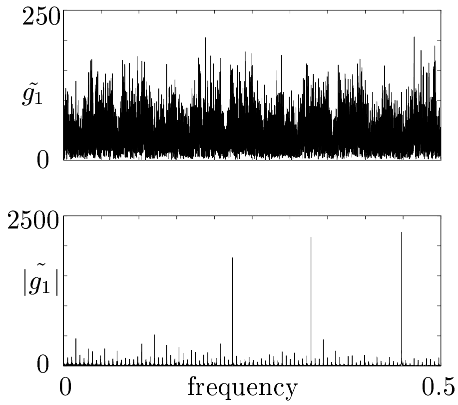

FIG. 5. Power spectrum of the evolution on the nontrivial fixed set, (a) of the coordinate g_1, and (b) of the absolute values $|g_1|$.

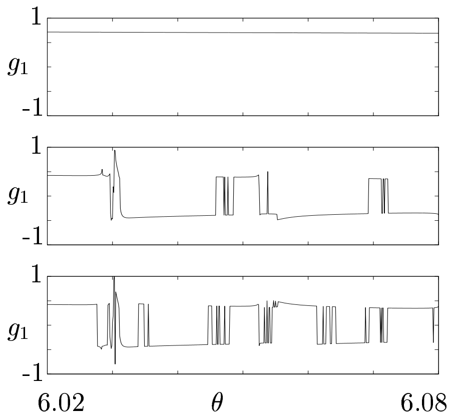

FIG. 4. Evolution of a set of initial conditions on the critical surface, parametrized by an angle θ varying over an interval $[\theta_1, \theta_2]$. We depict the projection of this set on the plane (θ, g_1) : (a) initial set, (b) after 100 iterations, and (c) after 350 iterations.

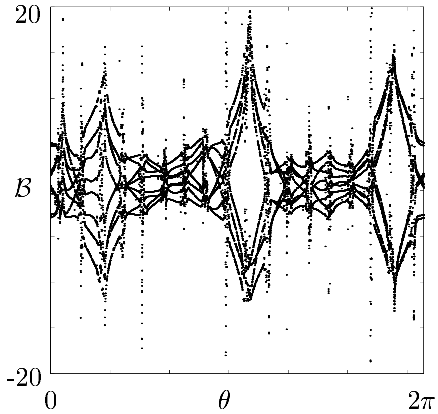

FIG. 6. Values of an observable $\mathcal{B}$ as a function of θ, on the critical attractor: it shows the eight branches of the attractor.

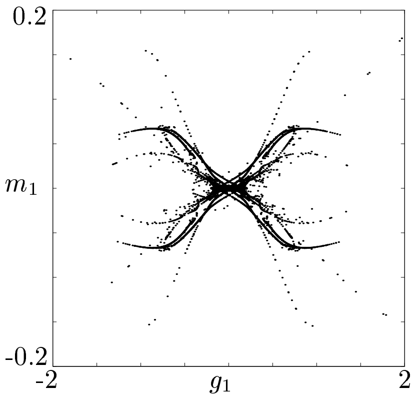

FIG. 7. Projection on the plane (g_1, m_1) of the critical attractor of the renormalization map.

[1] J.M. Greene, J. Math. Phys. **20**, 1183 (1979).
[2] L.P. Kadanoff, Phys. Rev. Lett. **47**, 1641 (1981).
[3] S.J. Shenker and L.P. Kadanoff, J. Stat. Phys. **27**, 631 (1982).
[4] R.S. MacKay, Physica **7D**, 283 (1983).
[5] R.S. MacKay, in *Renormalisation in Area-preserving Maps* (World Scientific, Singapore, 1993).
[6] M. Govin, C. Chandre, and H.R. Jauslin, Phys. Rev. Lett. **79**, 3881 (1997).
[7] C. Chandre, M. Govin, and H.R. Jauslin, Phys. Rev. E **57**, 1536 (1998).
[8] C. Chandre, M. Govin, H.R. Jauslin, and H. Koch, Phys. Rev. E **57**, 6612 (1998).
[9] J.J. Abad, H. Koch, and P. Wittwer, Nonlinearity **11**, 1185 (1998).
[10] J.M. Mao and R.H.G. Helleman, Nuovo Cimento **104B**, 177 (1989).
[11] R. Artuso, G. Casati, and D.L. Shepelyansky, Europhys. Lett. **15**, 381 (1991).
[12] R. Artuso, G. Casati, and D.L. Shepelyansky, Chaos, Solitons & Fractals **2**, 181 (1992).
[13] S. Tompaidis, Experimental Mathematics **5**, 197 (1996).
[14] S. Tompaidis, Experimental Mathematics **5**, 211 (1996).
[15] E.M. Bollt and J.D. Meiss, Physica D **66**, 282 (1993).
[16] S. Kurosaki and Y. Aizawa, Prog. Theor. Phys. **98**, 783 (1997).
[17] C. Chandre and H.R. Jauslin, Phys. Rev. Lett. **81**, 5125 (1998).
[18] C. Grebogi, E. Ott, S. Pelikan, and J.A. Yorke, Physica **13D**, 261 (1984).
[19] U. Feudel, J. Kurths, and A.S. Pikovsky, Physica D **88**, 176 (1995).
[20] G. Keller, Fundamenta Mathematicae **151**, 139 (1996).
[21] J. Stark, Physica D **109**, 163 (1997).
[22] R. Sturman and J. Stark, preprint (1999).
[23] S.R. McKay, A.N. Berker, and S. Kirkpatrick, Phys. Rev. Lett. **48**, 767 (1982).
[24] B. Derrida, J.P. Eckmann, and A. Erzan, J. Phys. A: Math. Gen. **16**, 893 (1983).
[25] O.E. Lanford, in *Statistical Mechanics and Field Theory: Mathematical Aspects*, edited by T.C. Dorlas, N.M. Hugenholtz, and M. Winnink (Springer-Verlag, Berlin,1986).
[26] O.E. Lanford, in *Nonlinear Evolution and Chaotic Phenomena*, edited by G. Gallavotti and P.F. Zweifel (Plenum Press, New York,1988).
[27] D.A. Rand, Proc. R. Soc. Lond. A **413**, 45 (1987).
[28] R.S. MacKay and I.C. Percival, Physica **26D**, 193 (1987).
[29] J.D. Farmer and I.I. Satija, Phys. Rev. A **31**, 3520 (1985).
[30] D.K. Umberger, J.D. Farmer, and I.I. Satija, Phys. Lett. **114A**, 341 (1986).
[31] I.I. Satija, Phys. Rev. Lett. **58**, 623 (1987).
[32] R.S. MacKay, J.D. Meiss, and J. Stark, Phys. Lett. A **190**, 417 (1994).
[33] C. Chandre and H.R. Jauslin, J. Math. Phys. **39**, 5856 (1998).
[34] S. Kim and S. Ostlund, Phys. Rev. A **34**, 3426 (1986).
[35] D.F. Escande and F. Doveil, J. Stat. Phys. **26**, 257 (1981).
[36] D.F. Escande, Phys. Rep. **121**, 165 (1985).
[37] C. Chandre, H.R. Jauslin, and G. Benfatto, J. Stat. Phys. **94**, 241 (1999).
[38] P. Grassberger and I. Procaccia, Phys. Rev. A **28**, 2591 (1983).
[39] J.P. Eckmann and D. Ruelle, Rev. Mod. Phys. **57**, 617 (1985).
[40] R.S. MacKay, in *Proceedings of the International Conference on Dynamical Systems and Chaos, Tokyo*, edited by Y. Aizawa, S. Saito, and K. Shiraiwa (World Scientific, Singapore, 1995).
[41] H. Koch, Erg. Theor. Dyn. Syst., to be published (1999).